



Real-Time Digital Control Using DSP of a Multiple Motors System

K. Boudjit kamelboudjit@gmail.com

Industrial Electrical Systems Laboratory

Department of Electrical Engineering

University of Science and Technology Houari Boumedienne (U.S.T.H.B.)

BP N°32 EL ALIA, Algiers, Algeria.

Abstract - A method for achieving the co-ordination and synchronisation of multiple motors on line using DSP is described. The co-ordination and synchronisation control of motion of multiple motors is a challenging problem, since the synchronisation of each individual motor can be influenced by many factors.

This paper presents the concept and implementation of a scheme that uses a real time control approach to realise drive synchronisation of the multiple motors. A new Master-Slave configuration is developed. Imperfect synchronisation can be corrected on-line using DSP. Also, this paper shows the advantages of using DSP controllers for such applications. Finally, experimental and simulation results are provided to validate the performance of the digital implementation.

Index terms - Synchronisation, Multiple-Motors, DSP, Master-Slave. Digital control.

I. INTRODUCTION

The highly competitive market coerces manufacturing industry towards the improvement of machine flexibility and productivity. A typical traditional machine design with mechanisms (such as gears, camshafts, linkages) has a number of disadvantages : extended part changeover time, inaccuracies due to wear, rudimentary motion profiles and the reliability of mechanical transmissions tends to be reduced by increases in machine speeds. Industry has been attracted by the possible replacement of the traditional machine with the system multiple motors [1]. The function that each drive performs is readily programmable. The drives are forced into coordination and synchronisation by some sort of software mechanism which are also implemented by programming [8].

Many manufacturing process require that constituent parts of a mechanism be synchronised. These processes would include any based on the manufacture or handling of sheet materials such as paper or rolled steel [6]. Traditionally processes would be synchronised through a mechanical transmission system consisting of a line-shaft, gearing, pullers, etc

Among the available software mechanisms, master/slave synchronisation is a widely used technique [1].

Some applications require the motion of the slave axes to follow the actual states of the master (such as in packaging, flying shears and other cyclic cutting applications), and this arrangement reduces the relative following-error more directly than some of alternative synchronisation mechanisms [1].

More recently there has been a large interest in electronic synchronisation, because it offers certain advantages in terms of flexibility and reliability. For example, where product specifications vary with the relative motion of constituent sections, this can be changed in software with a minimum of down time and possibly even online. The increases reliability has much to do with the removal of the mechanical transmission [7] [8].

With rapid developments of the system-on-chip, the high-performance digital processor (DSP) has become a popular area of research in the field of the digital control, for the drives because they exhibit high-speed performance, and combine peripheral circuits, memory and an optimized CPU structure on a single chip. In particular, a new-generation DSP controller TMS320F2812 provided by Texas Instruments, which provides the advantages of high speed (150MIPS), up to 128Kx16 flash, two set (total 12 lines) of PWM outputs, two sets (total 4 lines) of QEP inputs, a 16-channels 12-bit A/D converter (800 ns conversion time) and a 56-bits GPIO. Therefore, it is not only suitable multiple motor control, but also the complex algorithm, such as fuzzy control or neural network control, applied to servo-system to improve the dynamic performance become possible [2] [3].

This paper discusses an implementation where a continuously variable speed operation is provided for the multiple motors by using a single low cost DSP controller. These controllers implement variable speed drives with minimum external hardware thus increasing the reliability. A new master-slave control scheme using DSP is developed. Imprecise synchronisation can be corrected on-line; effectiveness of the DSP based "closed loop synchronisation mechanisms" demonstrated by comparison of simulation and experimental results. A complete hardware and software implementation with experimental results is presented.

II. MODELING AND CONTROL

An armature controlled DC motor with a load inertia mounted on its shaft is shown in figure 1.

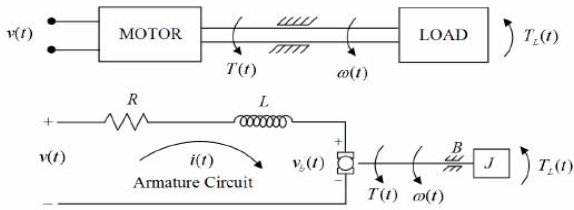


Fig1. Armature controlled DC motor and load.

The following equations govern the dynamics of this electromechanical system.

$$v(t) = Ri(t) + L \frac{d}{dt} i(t) + v_b(t), \quad (1)$$

$$v_b(t) = K_b \omega(t), \quad (2)$$

$$T(t) = K_T i(t), \quad (3)$$

$$J \frac{d}{dt} \omega(t) + B \omega(t) = T(t) + T_L(t). \quad (4)$$

Laplace transforming Eqs (1) (4) provides the basics for constructing the block diagram shown in figure 2.

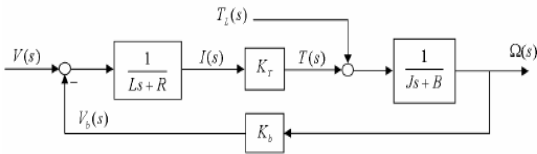


Fig.2. Block diagram of armature controlled DC motor.

The transfer function, $G_{\Omega}(s)$, $G_L(s)$ are obtained by block diagram of Mason's Gain formula. The results are:

$$G_{\Omega}(s) = \frac{\Omega(s)}{V(s)} \Big|_{T_L(s)=0} = \frac{\left(\frac{1}{Ls+R}\right) K_T \left(\frac{1}{Js+B}\right)}{1 + K_b \left(\frac{1}{Ls+R}\right) K_T \left(\frac{1}{Js+B}\right)}, \quad (5)$$

$$= \frac{K_T}{(Ls+R)(Js+B) + K_b K_T}, \quad (6)$$

$$G_L(s) = \frac{\Omega(s)}{T_L(s)} \Big|_{V(s)=0} = \frac{\left(\frac{1}{Js+B}\right)}{1 + K_b \left(\frac{1}{Ls+R}\right) K_T \left(\frac{1}{Js+B}\right)} \quad (7)$$

$$= \frac{Ls+R}{(Ls+R)(Js+B) + K_b K_T}. \quad (8)$$

By superposition, a property of linear systems, the motor response to combined changes in armature voltage and load torque is

$$\Omega(s) = G_{\Omega}(s)V(s) + G_L(s)T_L(s). \quad (9)$$

From Eq(9), the block diagram of the motor is as shown in figure 3.

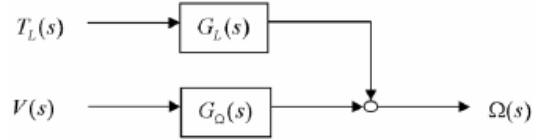


Fig.3. Block diagram of motor

The motor is modelled as a second order system with characteristics polynomial.

$$\Delta(s) = (Ls+R)(Js+B) + K_b K_T. \quad (10)$$

$$G_{\Omega}(s) = \frac{\frac{K_T}{JL}}{\left(s + \frac{R}{L}\right)\left(s + \frac{B}{J}\right) + \frac{K_b K_T}{JL}} = \frac{K \omega_n^2}{s^2 + 2\zeta \omega_n s + \omega_n^2}. \quad (11)$$

Solving for the steady-state gain (from voltage to angular speed) K_m , the natural frequency ω_n and the damping ratio ζ in terms of the motor parameters result.

$$K_m = \frac{K_T}{BR + K_b K_T}, \quad (12)$$

$$\omega_n = \left(\frac{BR + K_b K_T}{JL}\right)^{1/2}, \quad (13)$$

$$\zeta = \frac{(BL + JR)}{2[JL(BR + K_b K_T)]^{1/2}}. \quad (14)$$

The characteristic roots are obtained by solving $\Delta(s) = 0$.

$$s_1, s_2 = -\zeta \omega_n \pm \sqrt{\zeta^2 - 1} \omega_n. \quad (15)$$

The transfer function $G_{\Omega}(s)$ in Eq(11) is expressible in terms of the characteristic roots and motor time constants by

$$G_{\Omega}(s) = \frac{K \omega_n^2}{(s - s_1)(s - s_2)} = \frac{K \omega_n^2 \tau_1 \tau_2}{(\tau_1 s + 1)(\tau_2 s + 1)}, \quad (16)$$

It is common to ignore the armature inductance entirely and treat the motor as a first order component. This assumption introduce negligee error since the frequency components of the inputs $e_a(t)$ And $T_L(t)$ are well below the break frequency associated with the electrical time constant, $\omega_b = 1/\tau_e$.

The transfer function $G_{\Omega}(s)$ becomes a first order lag.

$$G_{\Omega}(s) = \frac{\Omega(s)}{V(s)} = \frac{K_m}{\tau_m s + 1}, \quad (17)$$

Where K_m is the steady-state motor gain (rpm/volt) in Eq (12) and τ_m is the motor time constant, same as the mechanical time constant. The same result follows directly from Eq (6) with $L=0$. The actual two dc motor is driven by a pulse width modulated (PWM) signal with period T and duty cycle $f = P / T$ like the on shown in figure 4.

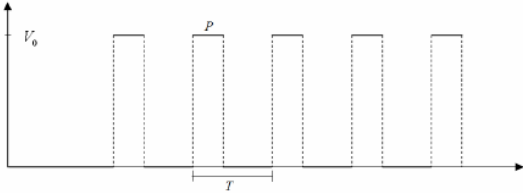


Fig.4. Pulse Width Modulated (PWM) Input to Motor
For a variable duty cycle $f(t)$, the effective voltage applied to the motor is:

$$v(t) = f(t)V_0 = \frac{P(t)}{T}V_0. \quad (18)$$

$$G_\Omega(s) = \frac{\Omega(s)}{V_0 F(s)}, \quad F(s) = L \{f(t)\}. \quad (19)$$

This leads to a new motor transfer function

$$\hat{G}_\Omega(s) = \frac{\Omega(s)}{F(s)} = V_0 G_\Omega(s) = V_0 \frac{\Omega(s)}{V(s)} = V_0 \frac{K_m}{\tau_m s + 1} = \frac{\hat{K}_m}{\tau_m s + 1} \quad (20)$$

Where $\hat{K}_m = V_0 K_m$ is the motor gain in rpm per% duty cycle.

The sensor gain is combined with the controller transfer function in figure 5 so that the command input may be shown in the same units as the control system output, i.e. rpm.

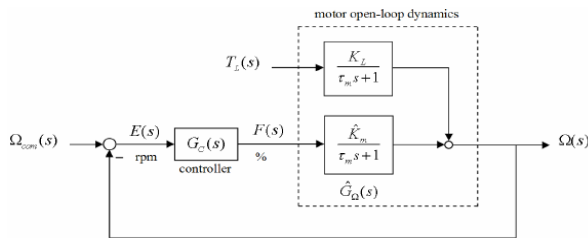


Fig.5. Closed-loop system for DC motor speed control
The closed-loop control system transfer function from command input $\Omega_{comm}(s)$ to angular speed $\Omega(s)$

$$T(s) = \frac{\Omega(s)}{\Omega_{comm}(s)} = \frac{G_C(s)\hat{G}_\Omega(s)}{1 + G_C(s)\hat{G}_\Omega(s)}, \quad (21)$$

$$= \frac{G_C(s) \frac{\hat{K}_m}{\tau_m s + 1}}{1 + G_C(s) \frac{\hat{K}_m}{\tau_m s + 1}} = \frac{\hat{K}_m G_C(s)}{\tau_m s + 1 + \hat{K}_m G_C(s)} \quad (22)$$

A conventional three term P-I-D controller will be used to control then motor speed. The continuous form is described by.

$$G_C(s) = \frac{\Delta F(s)}{E(s)} = K_p + \frac{K_I}{s} + K_D s. \quad (23)$$

$$T(s) = \frac{\Omega(s)}{\Omega_{comm}(s)} = \frac{\hat{K}_m \left(K_p + \frac{K_I}{s} + K_D s \right)}{\tau_m s + 1 + \hat{K}_m \left(K_p + \frac{K_I}{s} + K_D s \right)}, \quad (24)$$

$$= \frac{\hat{K}_m (K_D s^2 + K_p s + K_I)}{(\hat{K}_m K_D + \tau_m) s^2 + (\hat{K}_m K_p + 1) s + \hat{K}_m K_I}. \quad (25)$$

The initial design starts with a P-I controller ($K_D = 0$). The closed-loop transfer function reduces to.

$$T(s) = \frac{\Omega(s)}{\Omega_{comm}(s)} = \frac{\hat{K}_m (K_p s + K_I)}{\tau_m s^2 + (\hat{K}_m K_p + 1) s + \hat{K}_m K_I}, \quad (26)$$

And the characteristic polynomial is

$$\Delta(s) = \tau_m s^2 + (\hat{K}_m K_p + 1) s + \hat{K}_m K_I. \quad (27)$$

For a negative feedback control system with open-loop gain $K_p G(s)H(s)$, the characteristic equation is

$$\Delta(s) = 1 + K_p G(s)H(s) = 0. \quad (28)$$

$$\Delta(s) = s(\tau_m s + 1) + \hat{K}_m K_I + K_p \hat{K}_m s = 0. \quad (29)$$

$$1 + K_p \left[\frac{\hat{K}_m s}{s(\tau_m s + 1) + \hat{K}_m K_I} \right] = 0 \quad (30)$$

$$G(s)H(s) = \left[\frac{\hat{K}_m s}{s(\tau_m s + 1) + \hat{K}_m K_I} \right]. \quad (31)$$

Using the average Dc motor parameter values

$$(\hat{K}_m)_{ave} = 32.08 \frac{\text{rpm}}{\% \text{ change in duty cycle}}, \quad (\tau_m)_{ave} = 0.161 \text{ sec}$$

And choosing the integral constant $K_I = 1 \%$, produces the root-locus plot shown in figure 6.

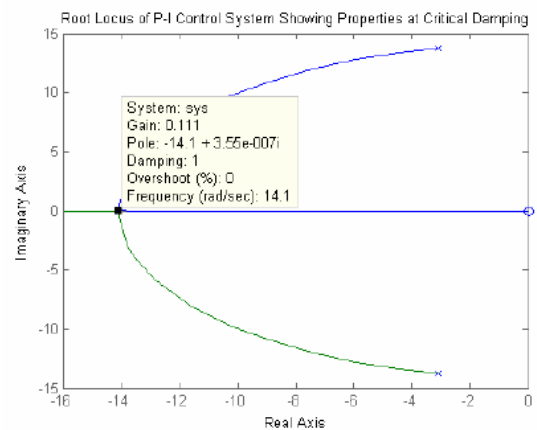


Fig.6. Root-locus for (P-I)

III. MULTIPLE MOTOR SPEED SYNCHRONISATIONS

Multiple motor synchronisations can be achieved by either the "equal-status" approach or "master-slave" approach [1]. In the equal-status approach, the synchronising controller treats each motor in a similar manner without favouring one axis over the

other. When the dynamics are significantly different among the axes in the group, the equal-status approach may not be the best because the synchronisation speed of the overall system is set by the slowest axis. In such a case, it is more appropriate to adopt the master-slave approach. The slow axis operates under conventional servo control and acts as the master for the faster axes [7] [8]. The figure 7, show the approach master-slave.

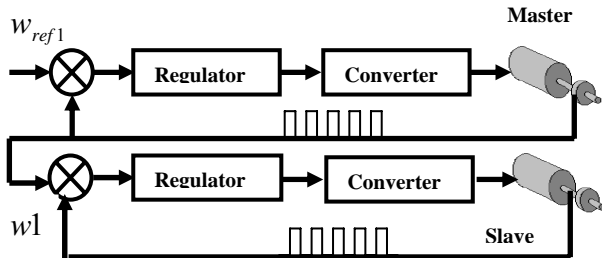


Fig.7. The Master-Slave approach

The master-slave technique is designed to reduce the synchronisation error under the assumption that the slaves can follow the master instantly.

IV. SIMULATION

The modelling developed in the part called “modelling control”, will be generalised for both motors.

The figure 8 show the model simulation of the two DC motors disposed in Master-Slave mode. Some results of continued simulation system in continue are presented in Figures (9) and (10). It illustrates the current and speed responses of the two DC motors respectively, when applied at two different times a variation of reference for the master motor.

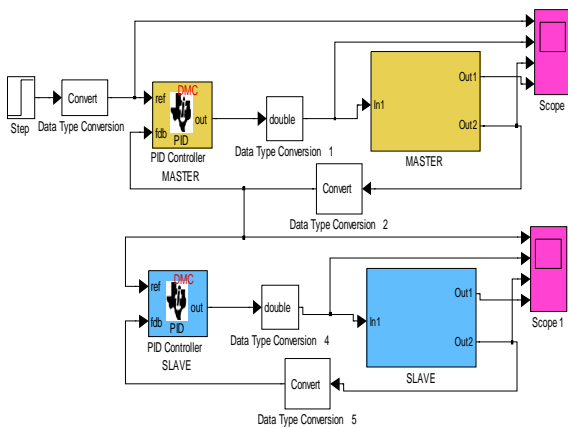


Fig.9. Model of simulation

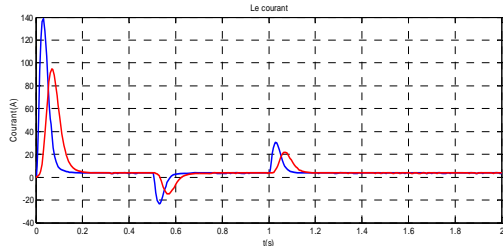


Fig.10. Current response of two motors

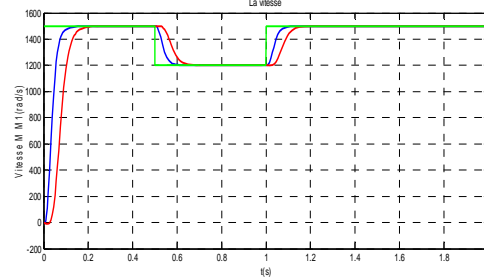


Fig.11. Speed response of two Motors

According to the simulation results, we note that synchronisation is achieved with a low error during a change applied to the master motor.

V. EXPERIMENTAL SET-UP

The experimental kit include two identical DC motors, they are rated for operating up to 24 Volts. They have a built-in encoder that outputs 72 pulses per revolution.

The DSP cannot directly drive the motor. Its PWM outputs can source about 4 mA of current. Each motor consumes about 100 mA when it’s supplied with 12 V. to provide this current; a motor driver integrated circuit is used. The L298 from ST Microelectronics is capable of powering two motors with up to 2 Amps each.

Some signal conditioning is required to properly interface the DSP board to the motor and encoder. A circuit board was assembled to address these issues. The encoder’s outputs are 5V signals. The DSP’s input pins are not tolerant of 5V levels. In fact, the entire chip can possibly be damaged by overvoltage signals. Through the motor driver chip provides some electrical isolation between the motor and DSP, an alternate solution with more protection was adopted. The PWM output on the DSP was connected to the input side of an optocoupler. The output of the optocoupler is connected to the control input of the motor driver chip. The motors and motor driver chips are powered from a different power supply than the DSP. Now, even if the two motors are drawing high levels of current, the DSP is unaffected. The block diagram for the entire system is shown in figure 12. Figure 13 shows the F2812 eZdsp board, motor driver board, interface board, and two motors.

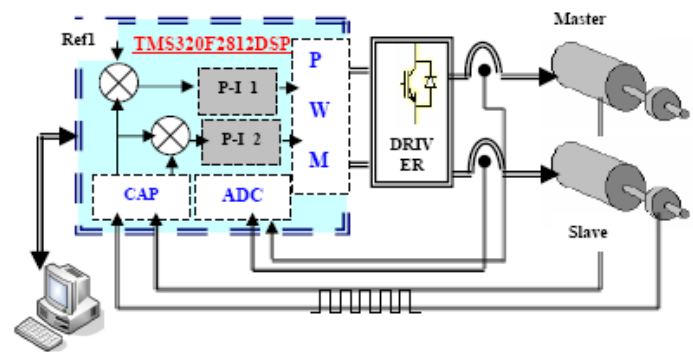


Fig.12. System Block Diagram

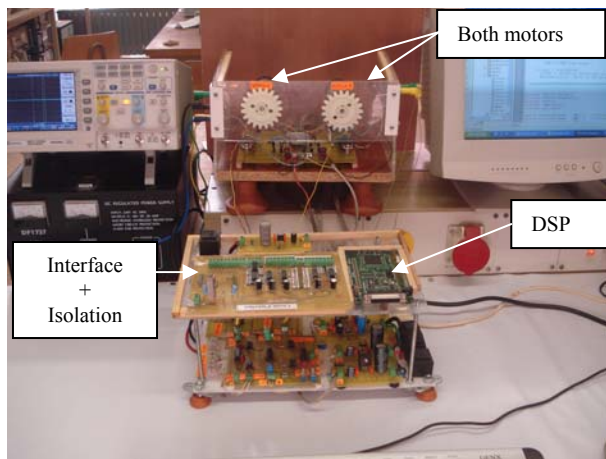


Fig.13. Experimental Setup

In the following, we presented a synchronisation speed control of two DC motors using the Master-Slave configuration. The basic principle of this control is the speed of both master and slave are measured and compared in such a way to get. Speed synchronisation of both motors regardless of the different modes of operation. This achieved using digital PI regulators on a DSP board (TMS320F2812).

Initially, our control system imposes a progressive ramp type start-up of both motors using PWM control signals generated by the DSP board. Next, each motor will require a speed regulation using a PI regulator.

A service routine interrupt that calls every $T_e = 0.1$ second for a calculation function of both PI, is used to implement our control system. With this, the first PI regulator (PI 1) “Master” compares the reference speed with the speed of the master motor, and its output is used to control in terms of PWM pulses the master motor.

The output speed of the master motor is then used as reference speed for the slave motor, and the second regulator PI 2 compares the measured speed of the slave motor with that of the master motor. And readjusts the PWM control signal in such a way to close the speed difference between both motors (Master-Slave).

The control system needs to be able to react to any fluctuation or change, in the master motor, so that the slave motor follows the master instantaneously.

A- Speed Measurement Module

For the measurement of the speed we use the unit capture (CAP) for DSP TMS320F2812. among the potential uses for the capture unit: low speed estimation of a rotating shaft. A potential advantage for low speed estimation is given when we use “time capture” (16-bit resolution) instead of position pulse counting (poor revolution in slow mode).

The feedback speed measurement is accomplished using T method, which is suitable for low speed measurement, as shows in figure 14.

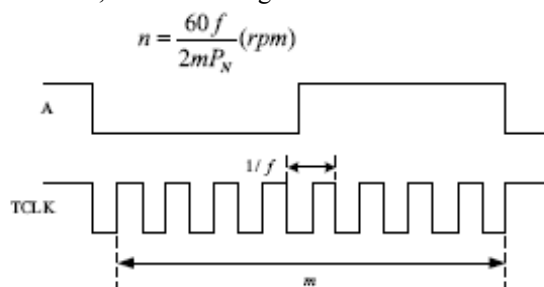


Fig.14. method of low speed measurement.

VI. EXPERIMENTAL RESULTS

All experiments presented in this paper have been done under. Constant voltage of 24 Volts and a speed reference of 1000 rpm.

Figure 15, illustrates the speed response of both motors without load.

Figure 16, shows the speed synchronisation and regulation of both motors without load.

Figure 17, illustrates the current response, of both motors without load and with regulation.

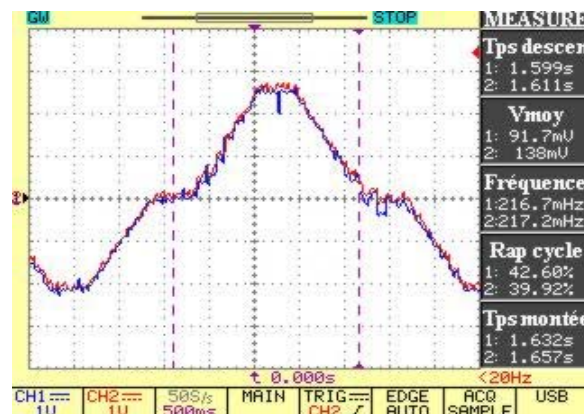


Fig.15. Speed response of both motors without load.

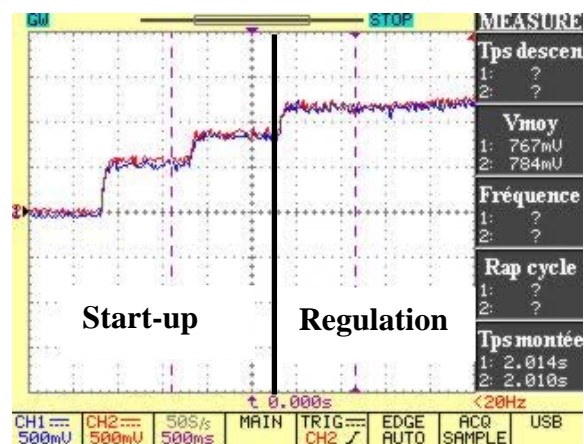


Fig.16. Speed synchronisation and regulation without load.

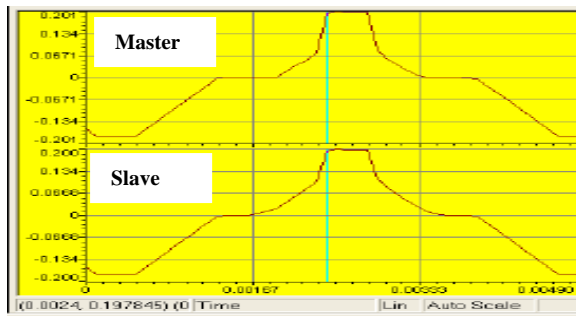


Fig.17. Current response of both motors without load.

Looking at figure 15 and 16 we can notice that both motors turn in both sense, knowing that the pulse width α varies from 05% up to 95 %, with $\Delta\alpha = 5\%$ every $T = 0.1s$. The final speed reached by both motors equals to 1230 rpm, and the final current reached is 180mA.

With this result, we observed that both motors follow the operation principles of a four quadrant chopper, where we have a current and speed inversion for both motor.

With this, the two motors synchronisation is achieved for a no-load operation.

For operation on load, we applied suddenly a load on the motor master and there is the evolution and response regulator for both motors.

Figures 18 and 19 illustrate the results obtained, respectively, the responses speed and current of both motors.

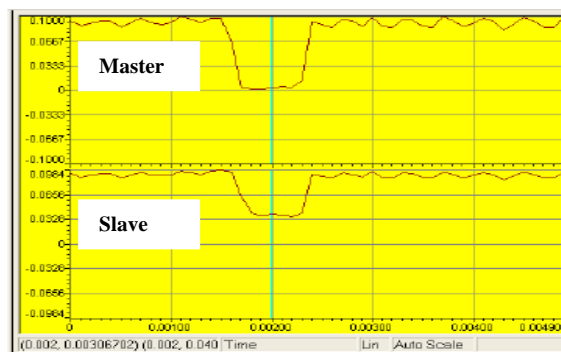


Fig.18. Speed response with load

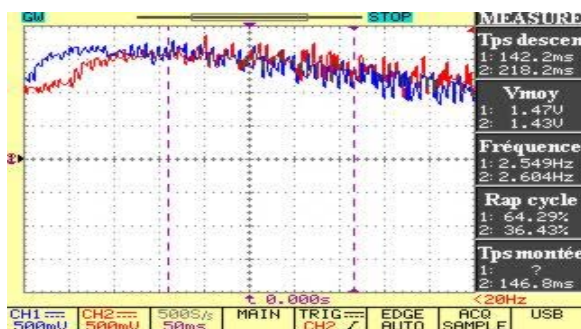


Fig.19. Current response with load.

According to the figures 17 and 18, we find that when applying a sudden load at the master, the slave follows the master. This confirms that our PI

editors involved in each interruption routine ($T = 0.1s$) to adjust the PWM signal has to move closer to the desired speed.

VII. CONCLUSION

A new coupling strategy for multi-axis motion synchronisation of independent multiple motors, which use DSP board, and real time control has been presented. This paper, the suitability of a new Master-Slave approach has been proven. Also this paper is to show that an advanced DSP controller can be a viable option for even most cost sensitive applications. This enables the user to take advantage of advanced algorithms to increase efficiency and also reduce system cost. The integrated power electronics peripherals available in these controllers also reduce the overall chip count of a complete system. The work described here still at a formative stage of development but the potential is clearly illustrated.

APPENDIX

Parameters of the both motors used in this paper.

Rated output	w	8.2
Rated torque	N.m	0.039
Rated speed	r/min	1500
Rated voltage	V	24
Rated current	A	0.3
Armature winding resistance	Ω	12.5
Armature inductance	mH	6
Torque constant	N.m/A	0.073

REFERENCES

- [1] P.R. Moore and C.M. Chen, "Fuzzy Logic Coupling and Synchronised Control of Multiple Independent Servo-Drives", Control Eng. Practice, Vol, 3, N°. 12, pp.1697-1708, 1995.
- [2] O. Pop, G. Chindris and A. Duff, "Using DSP Technology for True Sine PWM Generators for Power Inverters", Electronics Technology; Meeting the Challenges of Electronics Technology Progress, pp.141-146 Vol. 1,
- [3] Texas Instruments: TMS320F2812 Data Manual, Texas Instruments, (2004).
- [4] L. Osmancik, "The Four Quadrant Current Source Pulse Rectifier by DSP Controlled", Diploma Thesis, VSB-Technical University of Ostrava 2005.
- [5] L. Osmancik, "Digital Signal Processor TMS320F2812 and Its Application in Electric Drives", Applied Electronics 2006, Pilsen 6-7 September 2006.
- [6] Y.S. Kung and P.G. Huang, "High Performance Position Controller for PMSM Drives Based on TMS320F2812 DSP", 2004 IEEE CCA/ISIC/CACSD Joint Conferences, CCA Proceeding, Vol. I, pp. 290-295, September 2-4, 2004.
- [7] M. Tsai, Y. Kung, "Development of a Servo System for Linear X-Y Table Based on DSP Controller", IEEE, Proc. 1-4244-0726-5/06/S20.00 '2006 IEEE.
- [8] S. Wajih, "Controlling Multiple Motors Utilizing a Single DSP Controller", IEEE Transactions On Power Electronics, Vol. 18. N°. 1, January 2003.